Supporting Information

Rapid room temperature synthesis of red iridium(III) complexes containing four-membered Ir-S-C-S chelating ring for highly efficient OLEDs with EQE over 30%

Guang-Zhao Lu‡[a], Ning Su‡[a], Hui-Qing Yang[a], Qi Zhu[b], Wen-Wei Zhang[a], You-Xuan Zheng,*[a] Liang Zhou,*[b] Jing-Lin Zuo,*[a] Zhao-Xu Chen*[a] and Hong-Jie Zhang[b]

[a]*State Key Laboratory of Coordination Chemistry, Jiangsu Key Laboratory of Advanced Organic Materials, Collaborative Innovation Center of Advanced Microstructures, School of Chemistry and Chemical Engineering, Nanjing University, Nanjing 210093, P. R. China, E-mail: yxzheng@nju.edu.cn, zuojl@nju.edu.cn, zxchen@nju.edu.cn*

[b]*State Key Laboratory of Rare Earth Resource Utilization, Changchun Institute of Applied Chemistry, Chinese Academy of Sciences, Changchun 130022, P. R. China, E-mail: zhoul@ciac.ac.cn*

‡ *Lu and Su have the same contributions to this paper.*

Materials and Measurements.

All reagents and chemicals were purchased from commercial sources and used without further purification. ^{1}H NMR and ^{19}F NMR spectra were measured on a Bruker AM 400 spectrometer. Mass spectrometry spectra were obtained on an electrospray ionization mass spectrometer (LCQ fleet, Thermo Fisher Scientific) for ligands and high-resolution electrospray mass spectra (HRMS) was measured on G6500 from Agilent for complexes. Elemental analyses for C, H, and N were performed on an Elementar Vario MICRO analyzer. TG-DSC measurements were carried out on a DSC 823e analyzer (METTLER). Absorption and photoluminescence spectra were measured on a UV-3100 spectrophotometer and a Hitachi F-4600 photoluminescence spectrophotometer, respectively. The decay lifetimes were measured with an Edinburgh Instruments FLS-920 fluorescence spectrometer in degassed CH_2Cl_2 solution. The luminescence quantum efficiencies were calculated by comparison of the emission intensities of a standard sample (*fac*-Ir(ppy)$_3$) and the unknown sample.

Gibbs free energy calculation information.

All DFT computations were performed uisng B3LYP[1] functional and Lanl2DZ basis set[2] implemented in the Gaussian09 package[3]. The vibrational frequencies were calculated at the same level to guarantee all the located structures to be local minima on potential energy surfaces. The solvent effect was taken into consideration by the SMD model[4] in ethyl ether (Et_2O) solvent because its dielectric constant is similar to that of $EtOCH_2CH_2OH$, 13.38 F/m[5], and the structure of $EtOCH_2CH_2OH$ is analogous to Et_2O. The molecular structures were visualized by CYLview.[6]

X-ray Crystallography.

The single crystals of complexes were carried out on a Bruker SMART CCD diffractometer using monochromated Mo Kα radiation (λ = 0.71073 Å) at room temperature. Cell parameters were retrieved using SMART software and refined using SAINT on all observed reflections. Data were collected using a narrow-frame method with scan widths of 0.30° in ω and an exposure time of 10 s/frame. The highly redundant data sets were reduced using SAINT and corrected for Lorentz and polarization effects. Absorption corrections were applied using SADABS supplied by Bruker. The structures were solved by direct methods and refined by full-matrix least-squares on *F*2 using the program SHELXS-97. The positions of metal atoms and their first coordination spheres were located from direct-methods E-maps; other non-hydrogen atoms were found in alternating difference Fourier syntheses and least-squares refinement cycles and, during the final cycles, refined anisotropically. Hydrogen atoms were placed in calculated position and refined as riding atoms with a uniform value of Uiso.

Details of cyclic voltammetry measurements and theoretical calculations.

Cyclic voltammetry measurements were conducted on a MPI-A multifunctional electrochemical and chemiluminescent system (Xi'an Remex Analytical Instrument Ltd. Co., China) at room temperature, with a polished Pt plate as the working electrode, platinum thread as the counter electrode and Ag-$AgNO_3$ (0.1 M) in CH_2Cl_2 as the reference electrode, *tetra*-n-butylammonium perchlorate (0.1 M) was used as the supporting electrolyte, using Fc^+/Fc as the internal standard, the scan rate was 0.1 V/s. We perform theoretical calculations employing Gaussian09 software with B3LYP function. The basis set of 6-31G(d, p) was used for C, H, N, O, and F atoms while the LanL2DZ basis set was employed for Ir atoms. The solvent effect of CH_2Cl_2 was taken into consideration using conductor like polarizable continuum model (C-PCM).

OLEDs fabrication and measurement.

All OLEDs were fabricated on the pre-patterned ITO-coated glass substrate with a sheet resistance of 15 Ω/sq. The deposition rate for organic compounds is 1-2 Å/s. The phosphor and the host TCTA or 2,6DCzPPy were co-evaporated to form emitting layer from two separate sources. The cathode consisting of LiF / Al was deposited by evaporation of LiF with a deposition rate of 0.1 Å/s and then by evaporation of Al metal with a rate of 3 Å/s. The characteristic curves of the devices were measured with a computer which controlled KEITHLEY 2400 source meter with a calibrated silicon diode in air without device encapsulation. On the basis of the uncorrected PL and EL spectra, the Commission Internationale de l'Eclairage (CIE) coordinates were calculated using a test program of the Spectra scan PR650 spectrophotometer.

Table S1. The crystallographic data of $(4tfmpq)_2Ir(dipdtc)$ and $(4tfmpq)_2Ir(Czdtc)$.

	$(4tfmpq)_2Ir(dipdtc)$	$(4tfmpq)_2Ir(Czdtc)$
Formula	$C_{37}H_{30}F_6IrN_5S_2$	$C_{43}H_{24}F_6IrN_5S_2$
Formula weight	914.98	980.99
T (K)	296(2)	296(2)
Wavelength (Å)	0.71073	0.71073
Crystal system	Monoclinic	Monoclinic
Space group	$P2_1/n$	$P2_1/n$
a (Å)	13.9038(13)	8.4135(5)
b (Å)	34.924(3)	22.5714(13)
c (Å)	15.0724(15)	19.5667(12)
α (deg)	90.00	90.00
β (deg)	92.347(2)	95.3680(10)
γ (deg)	90.00	90.00
V (Å^3)	7312.7(12)	3699.5(4)
Z	8	4
ρ_{calcd} (g/cm^3)	1.662	1.761
μ (Mo Kα) (mm^{-1})	3.831	3.793
F (000)	3600	1920
Range of transm factors	1.473-25.010	1.381-25.004
Reflns collected	41033	20702

Unique(R_{int})	12875(0.0563)	6512(0.0625)
R_1^a, wR_2^b [I > 2s(I)]	0.0440, 0.0995	0.0386, 0.0805
R_1^a, wR_2^b (all data)	0.0689, 0.1127	0.0718, 0.0993
GOF on F^2	1.022	1.083

$R_1{}^a = \Sigma||F_o| - |F_c||/\Sigma|F_o|$. $wR_2{}^b = [\Sigma w(F_o{}^2 - F_c{}^2)^2/\Sigma w(F_o{}^2)]^{1/2}$

Table S2. Selected bond lengths and angles of $(4tfmpq)_2Ir(dipdtc)$ and $(4tfmpq)_2Ir(Czdtc)$.

	$(4tfmpq)_2Ir(dipdtc)$	$(4tfmpq)_2Ir(Czdtc)$
Selected Bonds	Bond length (Å)	Bond length (Å)
Ir-C(1)	2.002(7)	2.007(7)
Ir-C(2)	1.995(7)	2.012(7)
Ir-N(1)	2.045(5)	2.035(6)
Ir-N(2)	2.036(6)	2.037(5)
Ir-S(1)	2.4488(19)	2.4662(19)
Ir-S(2)	2.4499(19)	2.4318(19)
S(1)-C(3)	1.725(8)	1.710(7)
S(2)-C(3)	1.719(7)	1.702(7)
C(3)-N(3)	1.329(9)	1.367(9)
Selected angles	(°)	(°)
C(1)-Ir-N(1)	79.0(2)	78.5(3)
C(2)-Ir-N(2)	78.4(3)	78.5(3)
S(1)-Ir-S(2)	71.42(7)	70.59(6)
S(2)-C(3)-S(1)	112.2(4)	112.1(4)
C(3)-S(2)-Ir	88.2(3)	89.3(3)
C(3)-S(1)-Ir	88.1(3)	88.0(3)
N(3)-C(3)-S(1)	124.2(6)	125.0(6)

Table S3. The electronic cloud density distributions of three complexes.

Complex	Orbital	Energy/eV	Energy/eV	Composition (%)

		(Calculated)	(experimental)	Main ligand	Ir	Ancillary Ligand
$(4tfmpq)_2Ir(dipdtc)$	HOMO	-5.65	-5.44	47.90	39.42	12.67
	LUMO	-2.61	-3.19	94.35	3.45	2.20
$(4tfmpq)_2Ir(dpdtc)$	HOMO	-5.68	-5.50	43.55	47.66	8.79
	LUMO	-2.59	-3.20	93.51	4.08	2.41
$(4tfmpq)_2Ir(Czdtc)$	HOMO	-5.79	-5.61	45.49	45.85	8.66
	LUMO	-2.60	-3.22	93.33	4.13	2.54

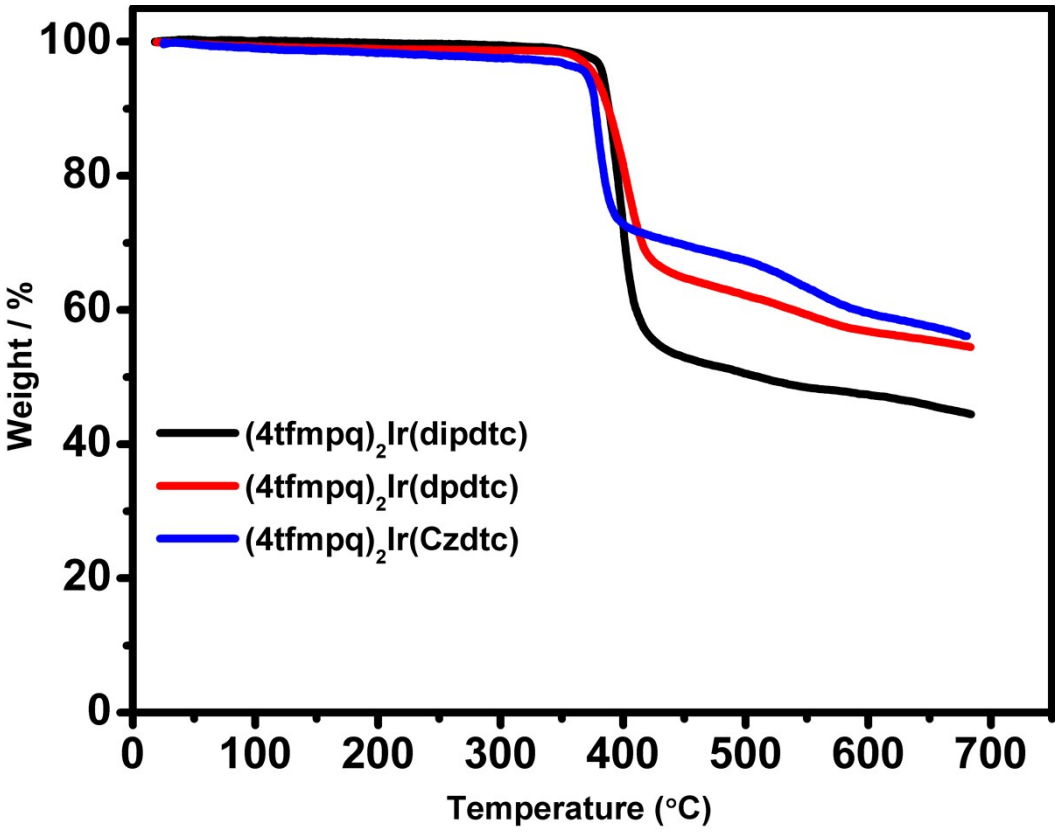

Fig. S1 The TG curves of $(4tfmpq)_2Ir(dipdtc)$, $(4tfmpq)_2Ir(dpdtc)$ and $(4tfmpq)_2Ir(Czdtc)$ complexes.

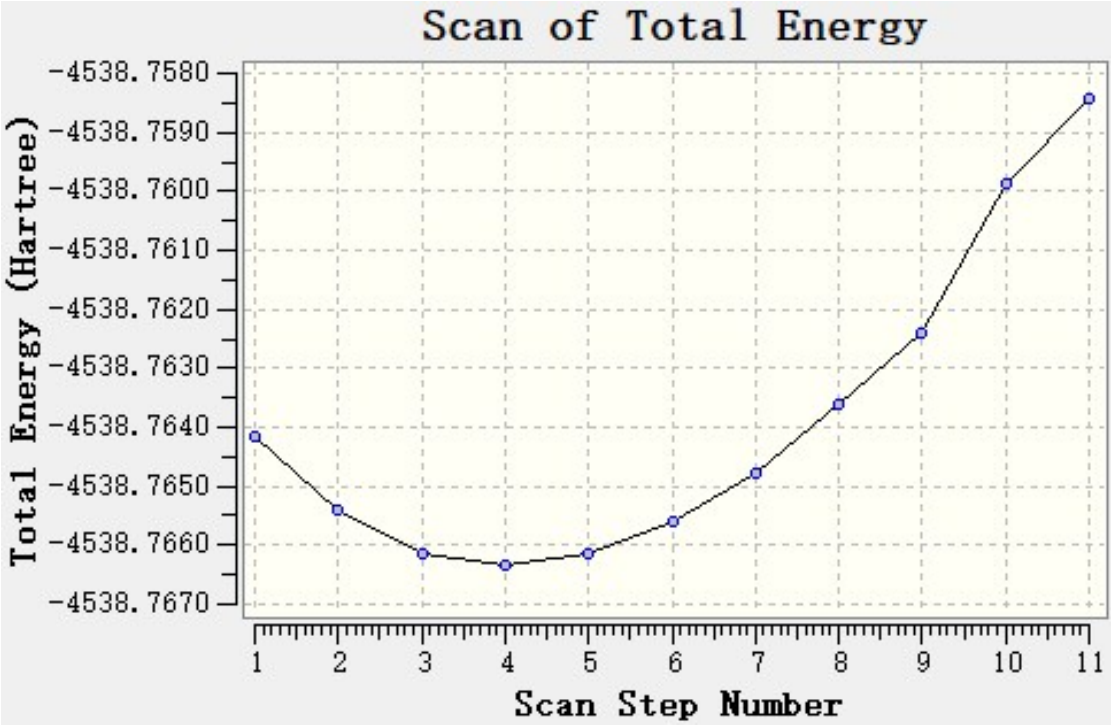

Fig. S2 The flexiblely scanning of the Ir-S bond length.

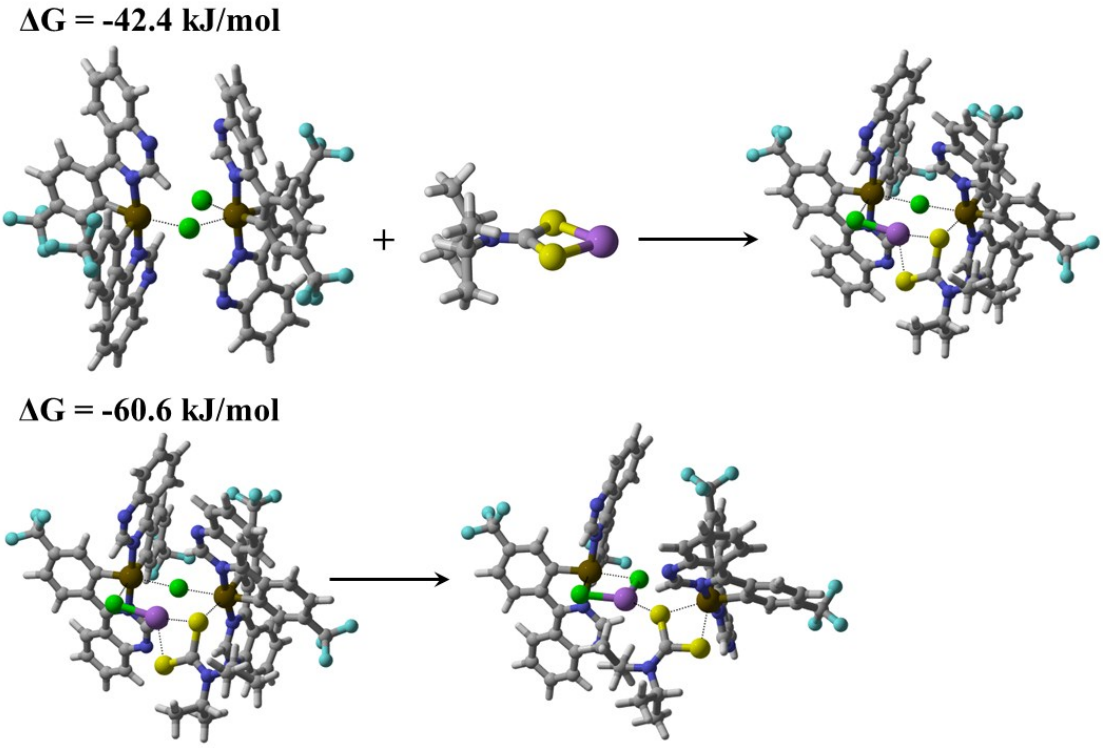

Fig. S3 The calculated free energy changes ΔG of formation the two S-Ir coordination bond.

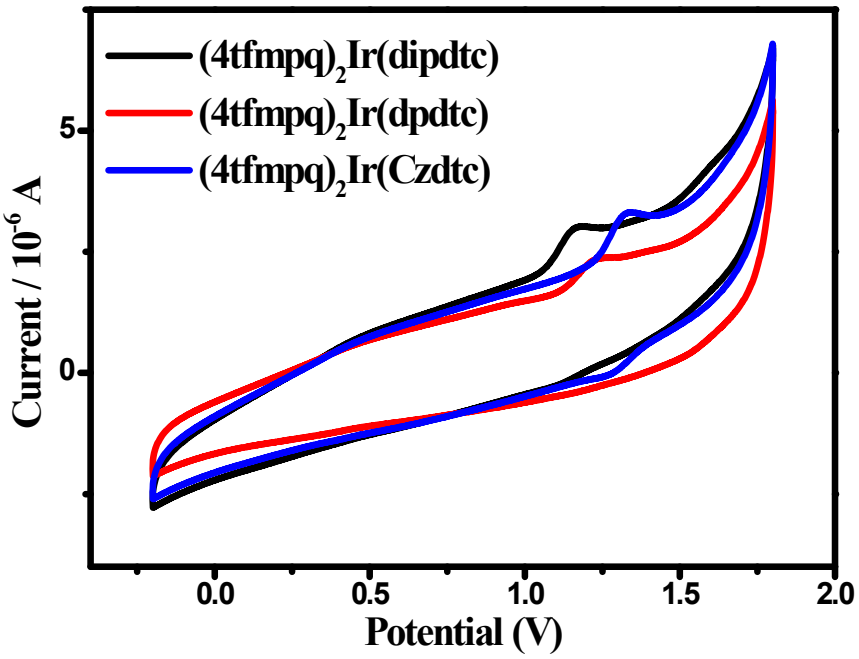

Fig. S4 Cyclic voltammograms of $(4tfmpq)_2Ir(dipdtc)$, $(4tfmpq)_2Ir(dpdtc)$ and $(4tfmpq)_2Ir(Czdtc)$ complexes.

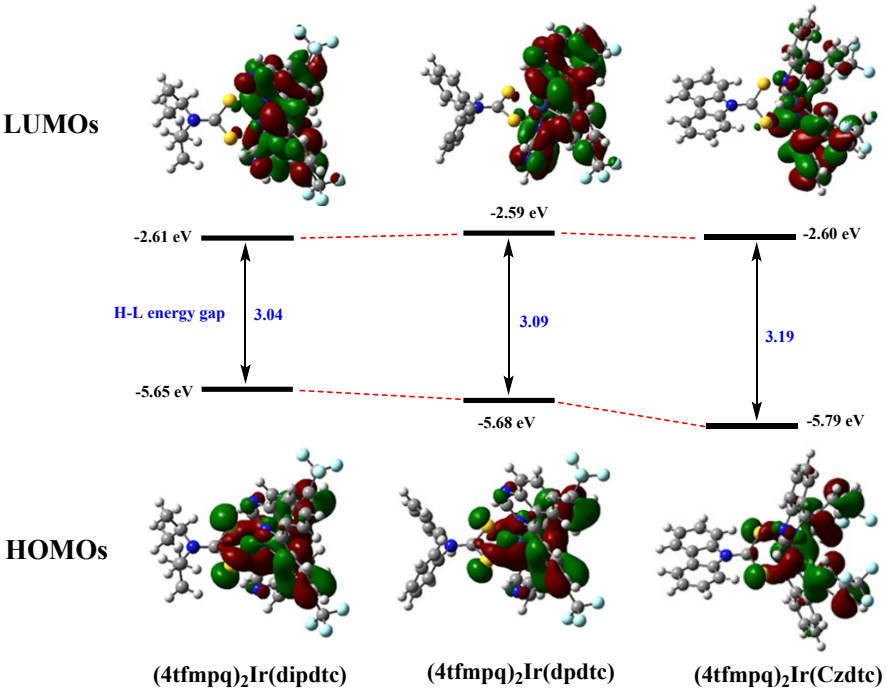

Fig. S5 The isodensity surface plots and HOMO/LUMO orbital levels of $(4tfmpq)_2Ir(dipdtc)$, $(4tfmpq)_2Ir(dpdtc)$ and $(4tfmpq)_2Ir(Czdtc)$ complexes.

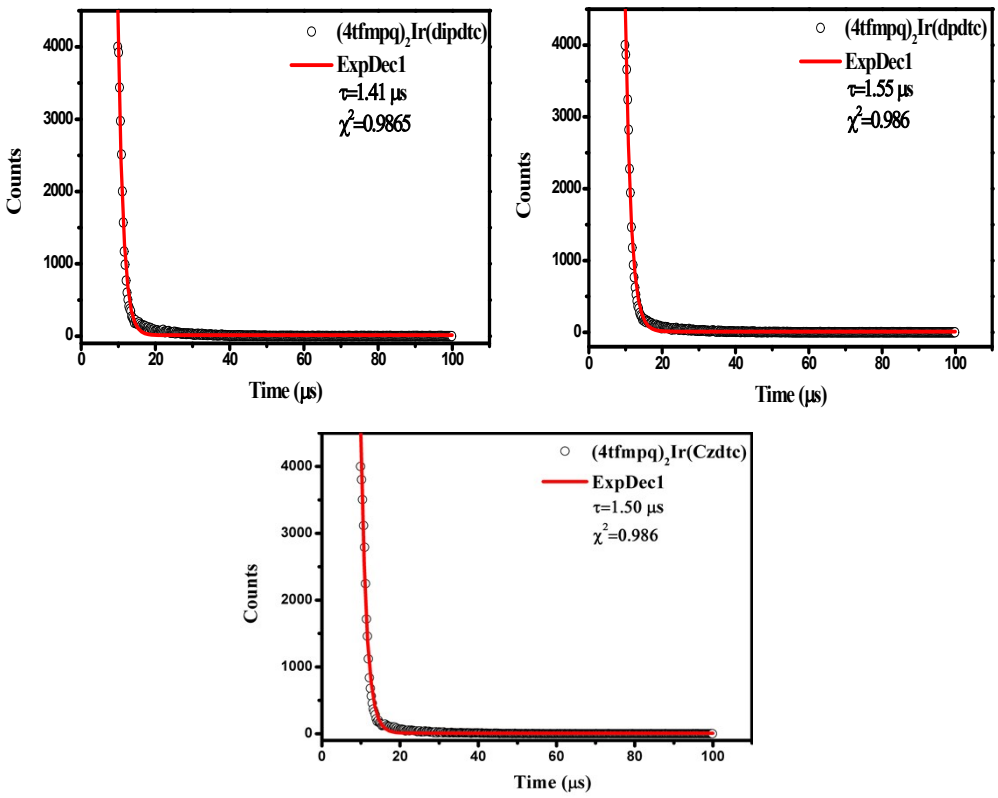

Fig. S6 The lifetime curves of $(4tfmpq)_2Ir(dipdtc)$, $(4tfmpq)_2Ir(dpdtc)$ and $(4tfmpq)_2Ir(Czdtc)$ complexes in degassed CH_2Cl_2 solution.

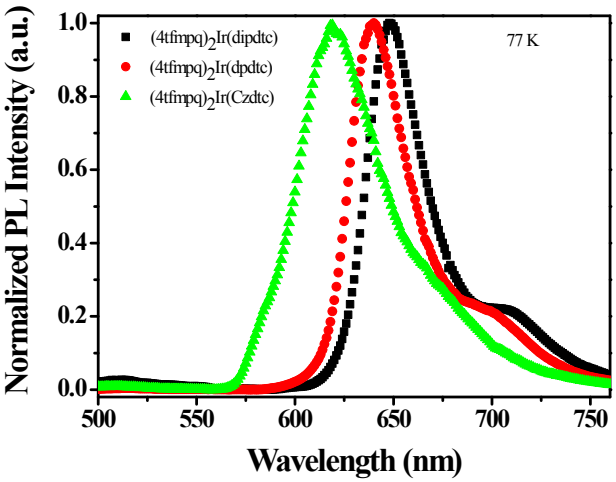

Fig. S7 The emission spectra of three complexes $(4tfmpq)_2Ir(dipdtc)$, $(4tfmpq)_2Ir(dpdtc)$ and $(4tfmpq)_2Ir(Czdtc)$ in degassed dichloromethane (5×10^{-5} M) at 77K.

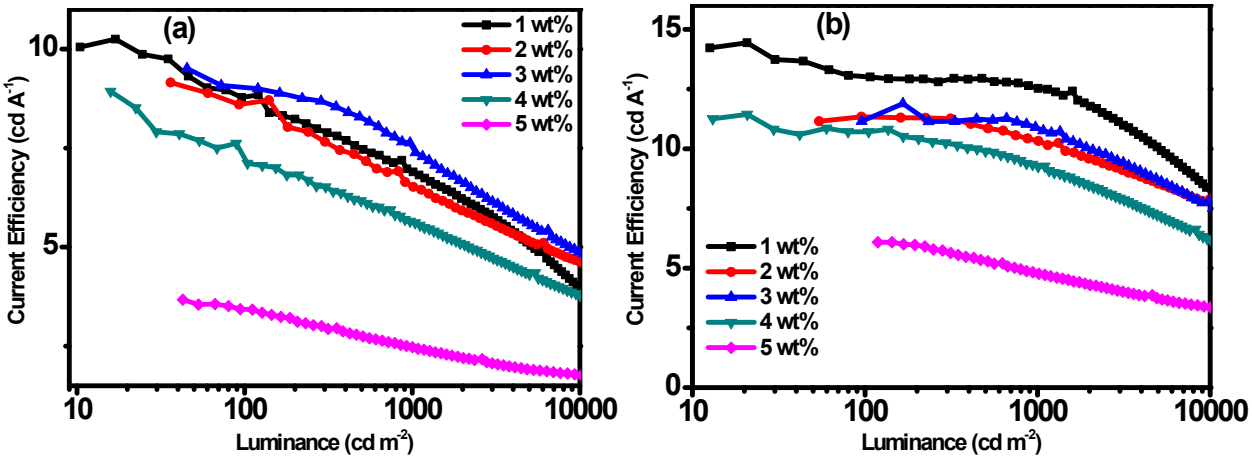

Fig. S8 Current efficiency versus luminance of different doped concentrations for $(4tfmpq)_2Ir(dipdtc)$ based devices: (a) single-emissive-layer and (b) double-emissive-layer.

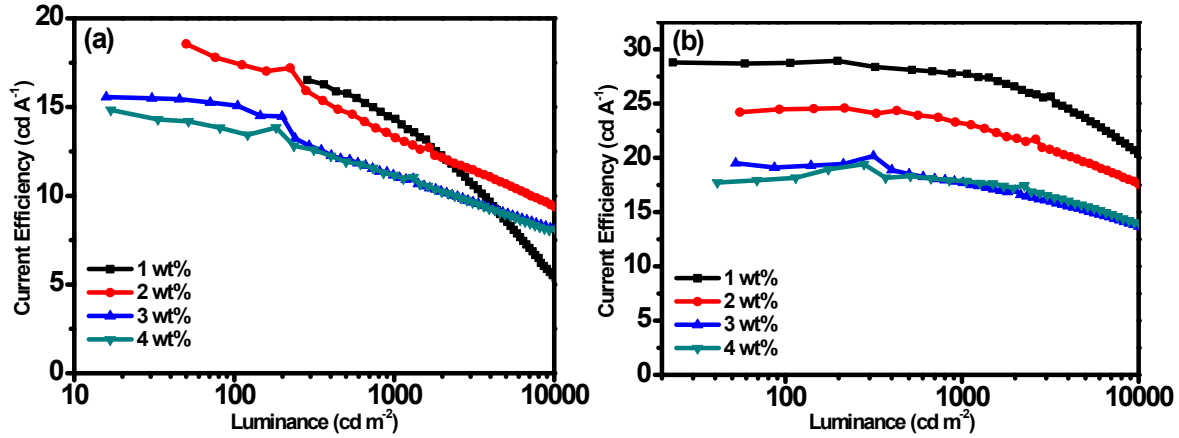

Fig. S9 Current efficiency versus luminance of different doped concentrations for $(4tfmpq)_2Ir(dpdtc)$ based devices: (a) single-emissive-layer and (b) double-emissive-layer.

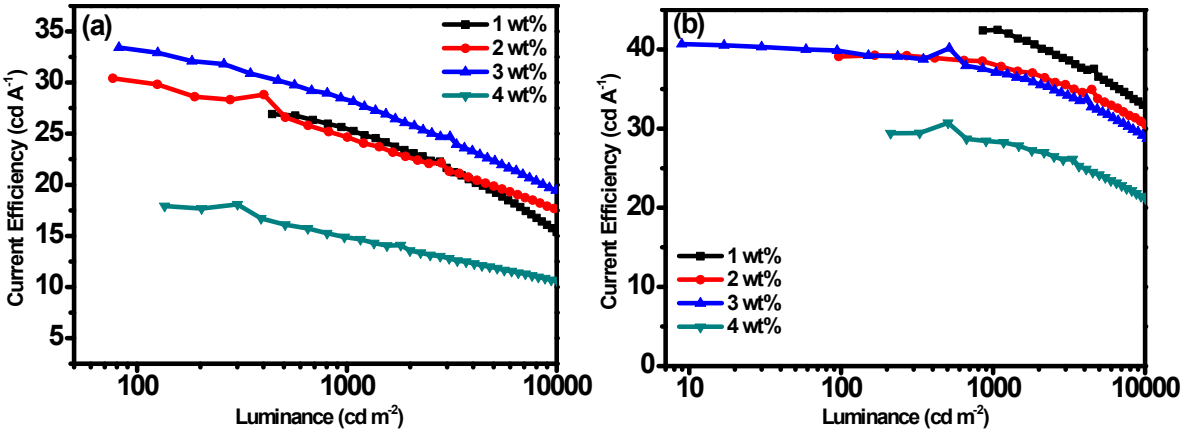

Fig. S10 Current efficiency versus luminance of different doped concentrations for $(4tfmpq)_2Ir(Czdtc)$ based devices: (a) single-emissive-layer and (b) double-emissive-layer.

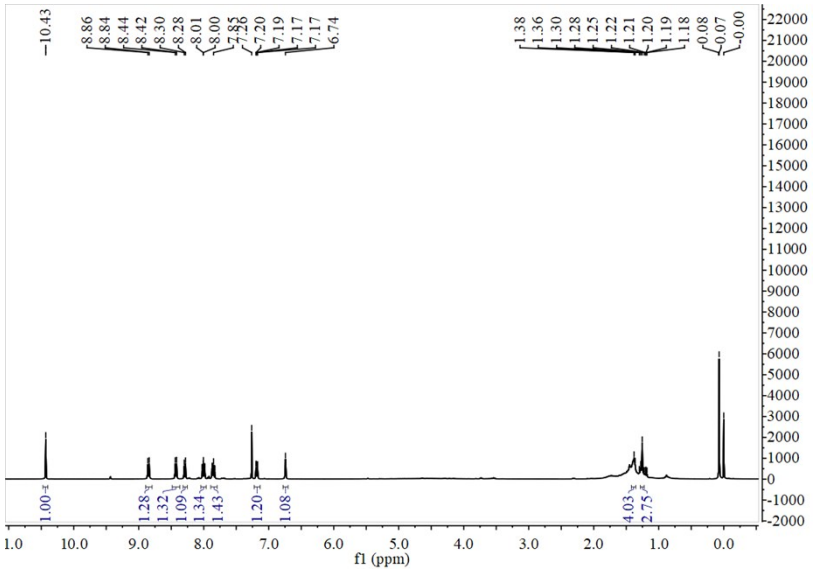

Fig. S11 ^{1}H NMR spectrum of $(4tfmpq)_2Ir(dipdtc)$.

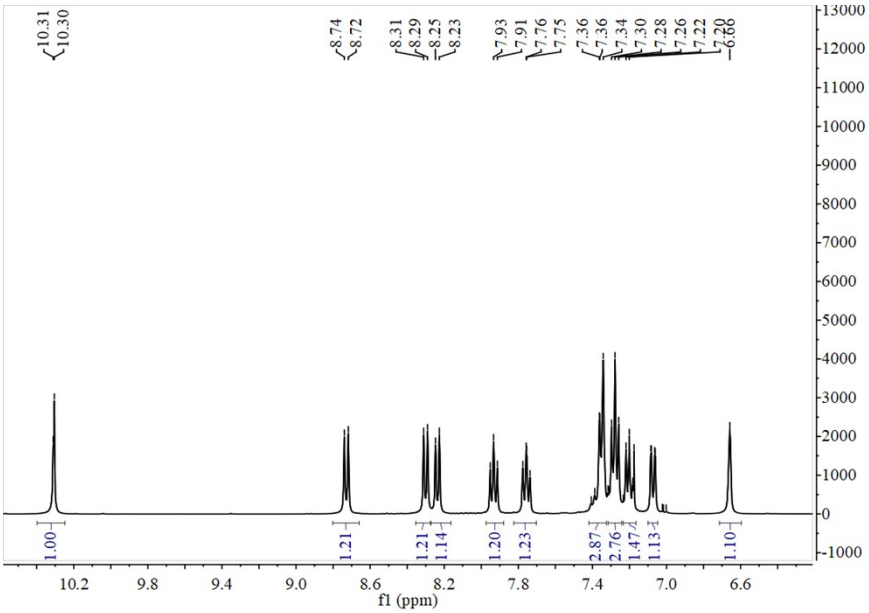

Fig. S12 ^{1}H NMR spectrum of $(4tfmpq)_2Ir(dpdtc)$.

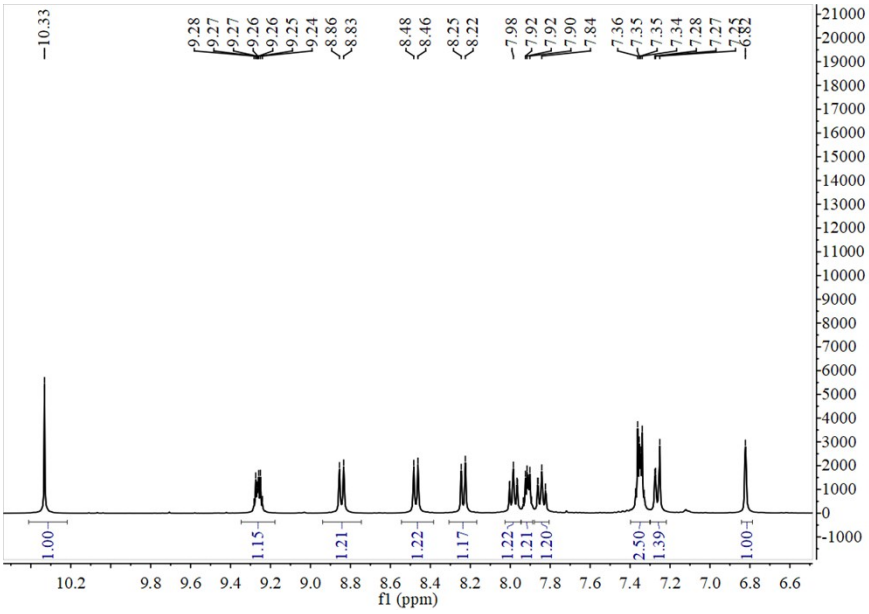

Fig. S13 ^{1}H NMR spectrum of $(4tfmpq)_2Ir(Czdtc)$.

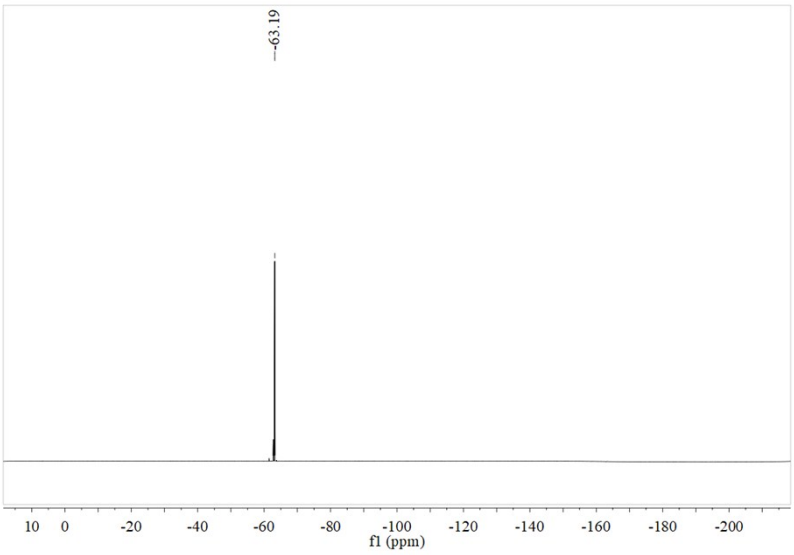

Fig. S14 ^{19}F NMR spectrum of $(4tfmpq)_2Ir(dipdtc)$.

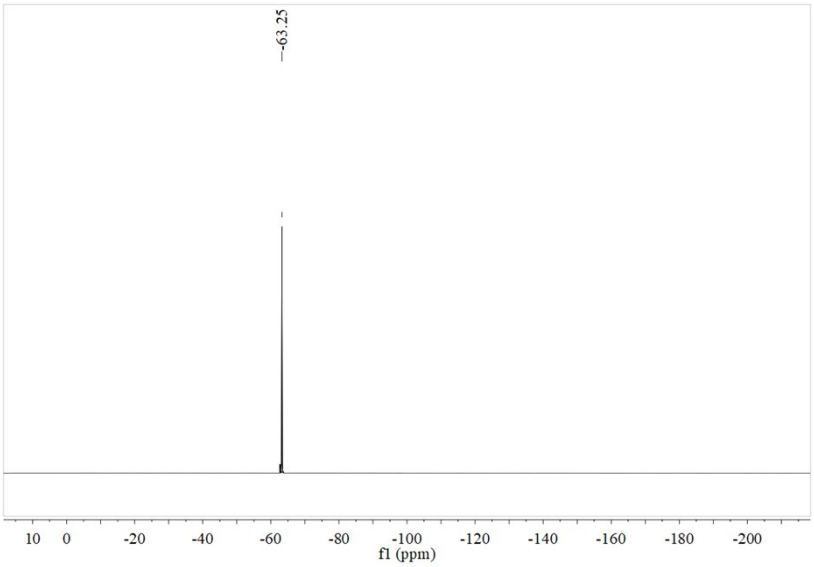

Fig. S15 ^{19}F NMR spectrum of $(4tfmpq)_2Ir(dpdtc)$.

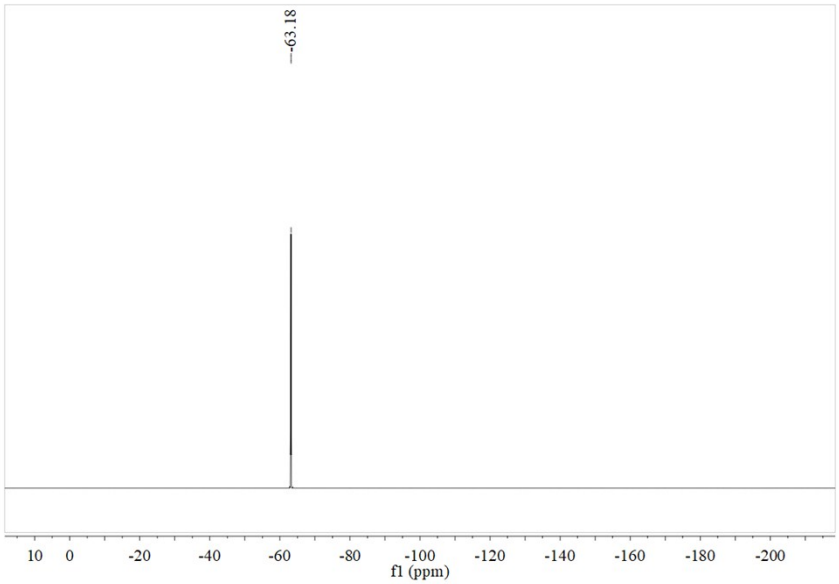

Fig. S16 ^{19}F NMR spectrum of $(4tfmpq)_2Ir(Czdtc)$.

Notes and References

1 A. D. Becke, *J. Chem. Phys*., 1993, **98**, 5648.

2 P. J. Hay and W. R. J. Wadt, *Chem. Phys.*, 1985, **82**, 270.

3 M. J. Frisch, G. W. Trucks, H. B. Schlegel, G. E. Scuseria, M. A. Robb, J. R. Cheeseman, G. Scalmani, V. Barone, B. Mennucci, G. A. Petersson, H. Nakatsuji, M. Caricato, X. Li, H. P. Hratchian, A. F. Izmaylov, J. Bloino, G. Zheng, J. L. Sonnenberg, M. Hada, M. Ehara, K. Toyota, R. Fukuda, J. Hasegawa, M. Ishida, T. Nakajima, Y. Honda, O. Kitao, H. Nakai, T. Vreven, J. A. Montgomery Jr., J.E. Peralta, F. Ogliaro, M. Bearpark, J. J. Heyd, E. Brothers, K. N. Kudin, V. N. Staroverov, R. Kobayashi, J. Normand, K. Raghavachari, A. Rendell, J. C. Burant, S. S. Iyengar, J. Tomasi, M. Cossi, N. Rega, J. M. Millam, M. Klene, J. E. Knox, J. B. Cross, V. Bakken, C. Adamo, J. Jaramillo, R. Gomperts, R. E. Stratmann, O. Yazyev, A. J. Austin, R. Cammi, C. Pomelli, J. W. Ochterski, R. L.Martin, K. Morokuma, V. G. Zakrzewski, G. A. Voth, P. Salvador, J. J. Dannenberg, S. Dapprich, A. D. Daniels, O. Farkas, J. B. Foresman, J. V. Ortiz, J. Cioslowski and D. J. Fox, Gaussian 09, Revision A.01, Gaussian, Inc., Wallingford, CT, 2009.

4 A.V. Marenich, C.J. Cramer and D.G. Truhlar, *J. Phys. Chem. B*, 2009, **113**, 6378.

5 G. Douheret and A. Pal, *J. Chem. Eng. Data*, 1988, **33**, 40.

6 C. Y. Legault, Université de Sherbrooke, CY Lview, 1.0b, 2009.